Supporting Information

Direct imaging of visible-light-induced one-step charge separation at the chromium(III) oxide–strontium titanate interface

Aufandra Cakra Wardhana, [a] Sou Yasuhara, [a] Min-Wen Yu, [b, c] Akira Yamaguchi, [a] Tadaaki Nagao,[b, d] Satoshi Ishii*,[b, e] and Masahiro Miyauchi*[a]

[a] Department of Materials Science and Engineering, Tokyo Institute of Technology, 2-12-1 Ookayama, Meguro-ku, Tokyo 152-8552, Japan
[b] International Center for Materials Nanoarchitectonics (MANA), National Institute for Materials Science (NIMS), 1-1 Namiki, Tsukuba, Ibaraki 305-004, Japan
[c] College of Photonics, National Chiao Tung University, 301 Gaofa 3rd road, Tainan 71150, Taiwan
[d] Department of Condensed Matter Physics, Graduate School of Science, Hokkaido University, Sapporo 060-0808, Japan
[e] Faculty of Pure and Applied Physics, University of Tsukuba, Tsukuba, Ibaraki 305-8557, Japan

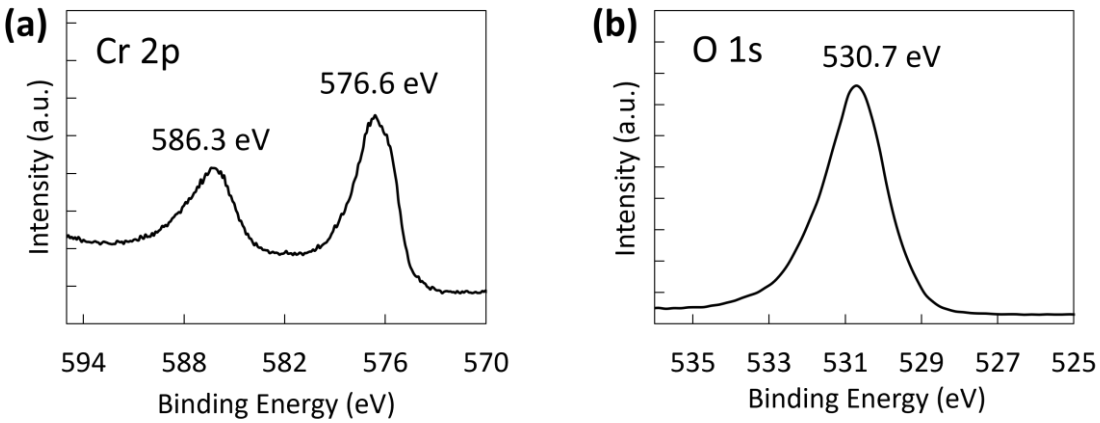

Figure S1. XPS spectra of Cr 2p and O 1s from Cr_2O_3 thin film.

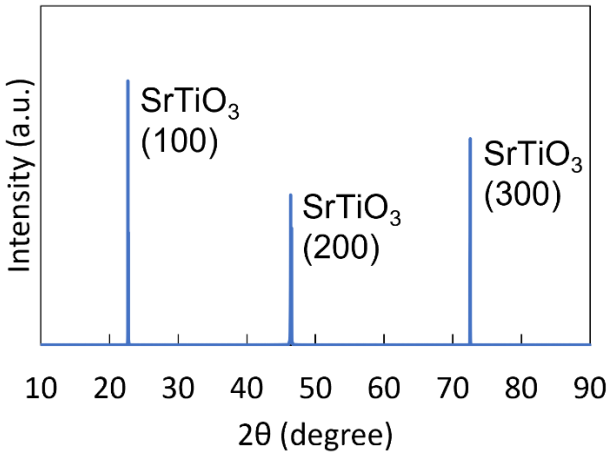

Figure S2. XRD pattern of $Cr_2O_3/SrTiO_3$ thin film system.

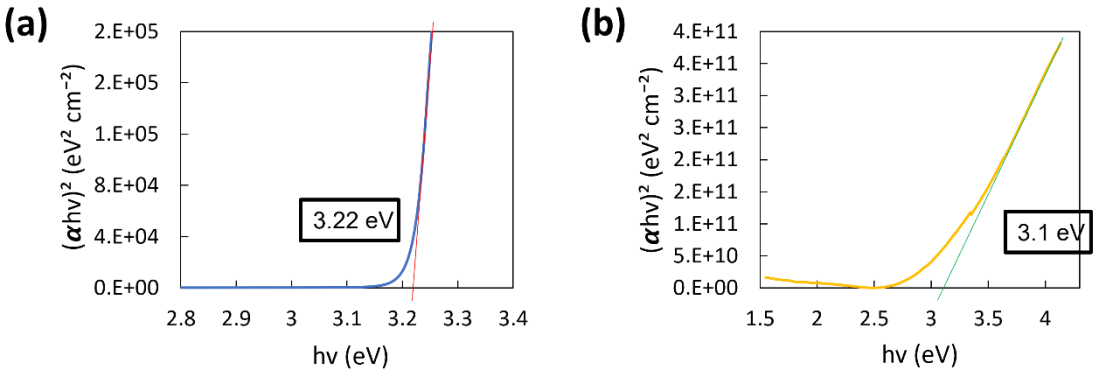

Figure S3. Tauc plots for $SrTiO_3$ substrate and Cr_2O_3 coated quartz glass.

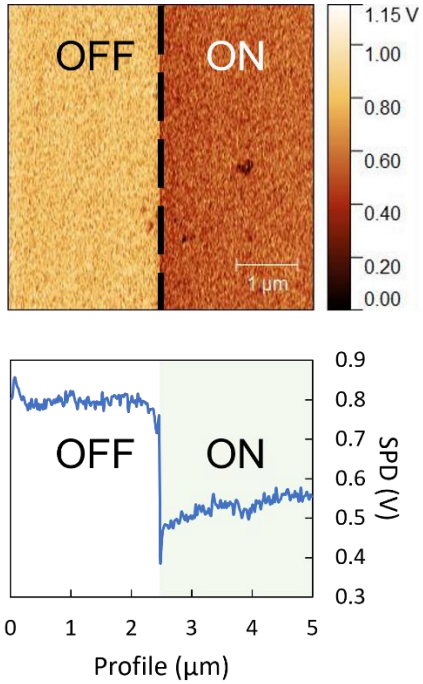

Figure S4. Surface potential mapping on Cr_2O_3/Nb-doped $SrTiO_3$ under light off and on. The light source used in this case was a 470 nm laser.

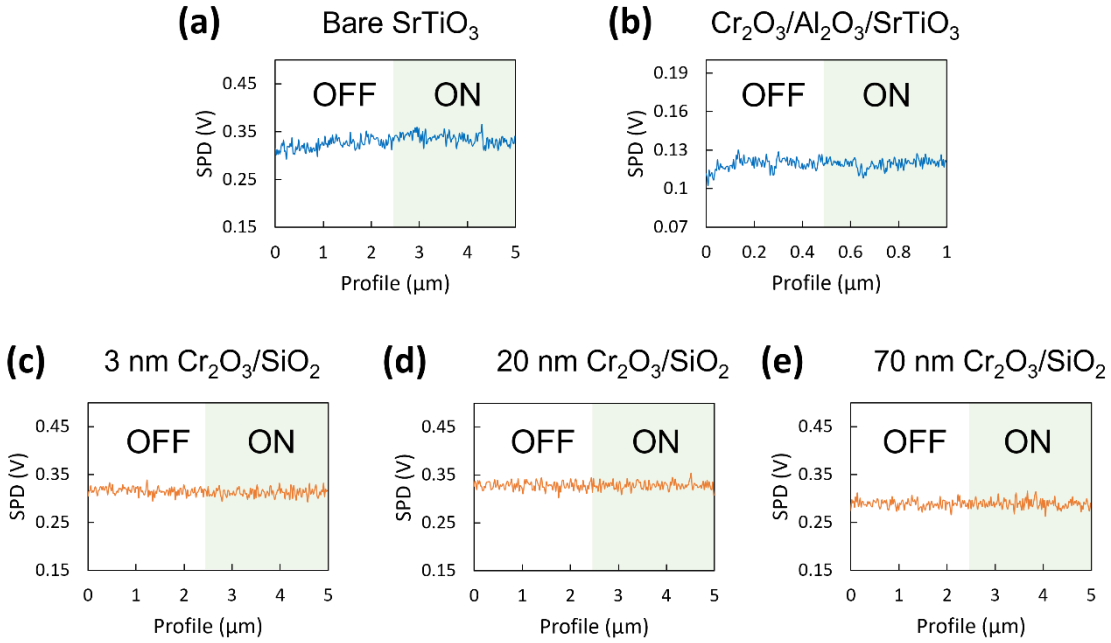

Figure S5. Surface potential mapping on $SrTiO_3$, $Cr_2O_3/Al_2O_3/SrTiO_3$, Cr_2O_3/SiO_2 as control experiments under light off and on. The light source used in this case was a 405 nm laser.

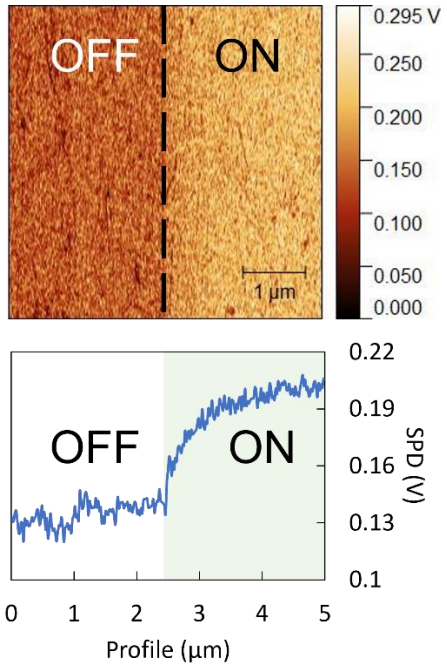

Figure S6. Surface potential mapping on Cr_2O_3/SiO_2 under light off and on. The light source used in this case was a UV LED (365 nm).

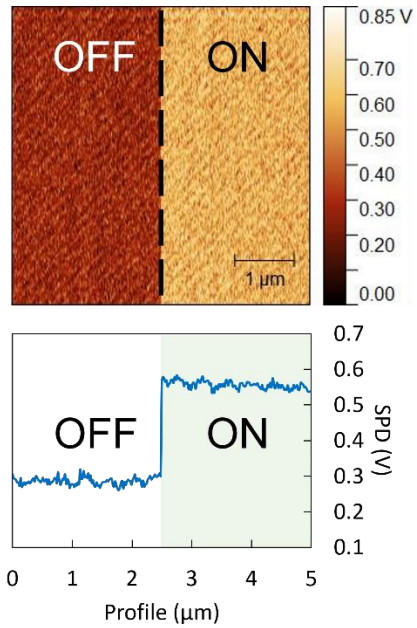

Figure S7. Surface potential mapping on $SrTiO_3$ (100) substrate under light off and on. The light source used in this case was a UV LED (365 nm).

In this case, the Cr_2O_3 thin film and $SrTiO_3$ substrate exhibited positive shifts of SPD. Holes

might accumulate on the surface due to the upward band bending. In addition, electrons accumulation on the surface is another possibility as various trap states might exist, including surface oxygen vacancy.[1–3]

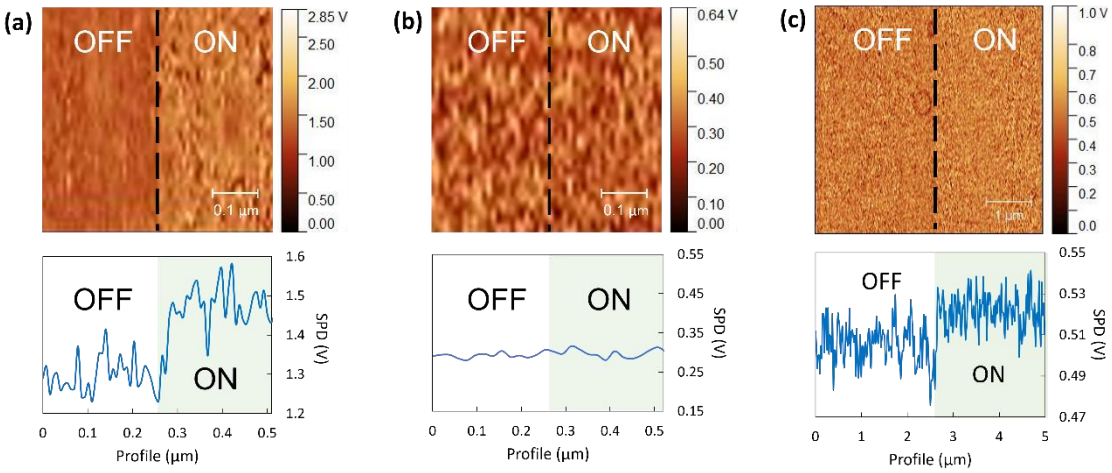

Figure S8. Surface potential mapping on 3 nm $CuO_x/SrTiO_3$ (a) and 3 nm CuO_x/SiO_2 (b) and 20 nm CuO_x/SiO_2 (c) under light off and on. The light source used in this case was a 470 nm laser.

The band gap of CuO_x thin film is around 1.4 eV, which can be excited by a 470 nm laser. In this study, we prepared an amorphous CuO_x thin film on a $SrTiO_3$ substrate by the same method and condition in our previous work.[4] The KPFM observation on 3 nm $CuO_x/SrTiO_3$ (Figure S8a) showed an upshift of SPD upon 470 nm irradiation, whereas 3 nm CuO_x/SiO_2 (Figure S8b) did not show any shift. However, we found that 20 nm CuO_x/SiO_2 showed an SPD upshift during 470 nm (Figure S8c). These results revealed that the bandgap excitation in CuO_x under its ultrathin form (3 nm) did not contribute to the SPD shift.

In the present study, the excitation state of the thicker CuO_x thin film, as shown by the SPD upshift, agrees with our photodeposited Ag in the previous report.[5] That is, photodeposited Ag particles on the 100 nm CuO thin film surface were clearly observed compared to that 6 nm CuO thin film.

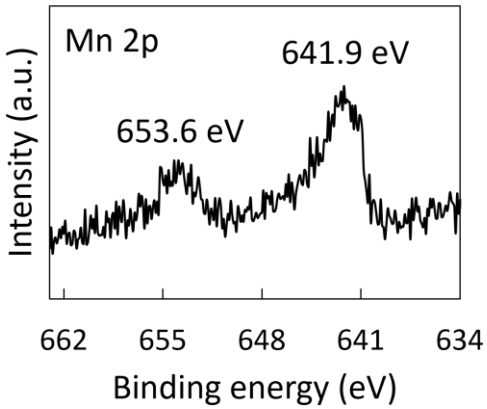

Figure S9. XPS spectrum of Mn 2p from the photodeposited MnO_x on $Cr_2O_3/SrTiO_3$.

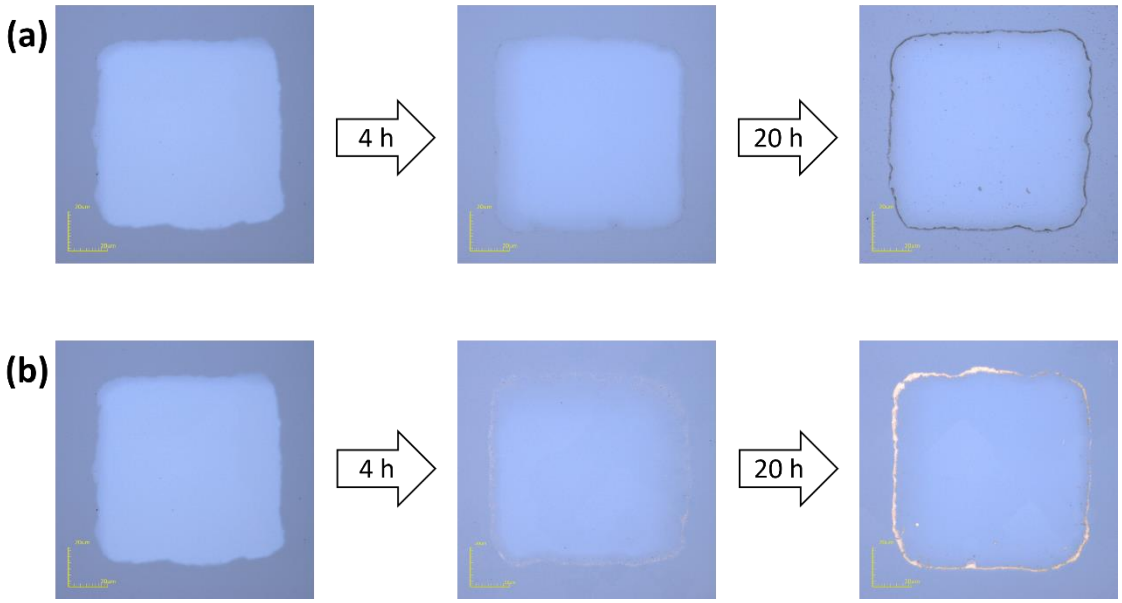

Figure S10. The growth of the photodeposited MnO_x (a) and Au (b) on $Cr_2O_3/SrTiO_3$ after 4 and 20 hours.

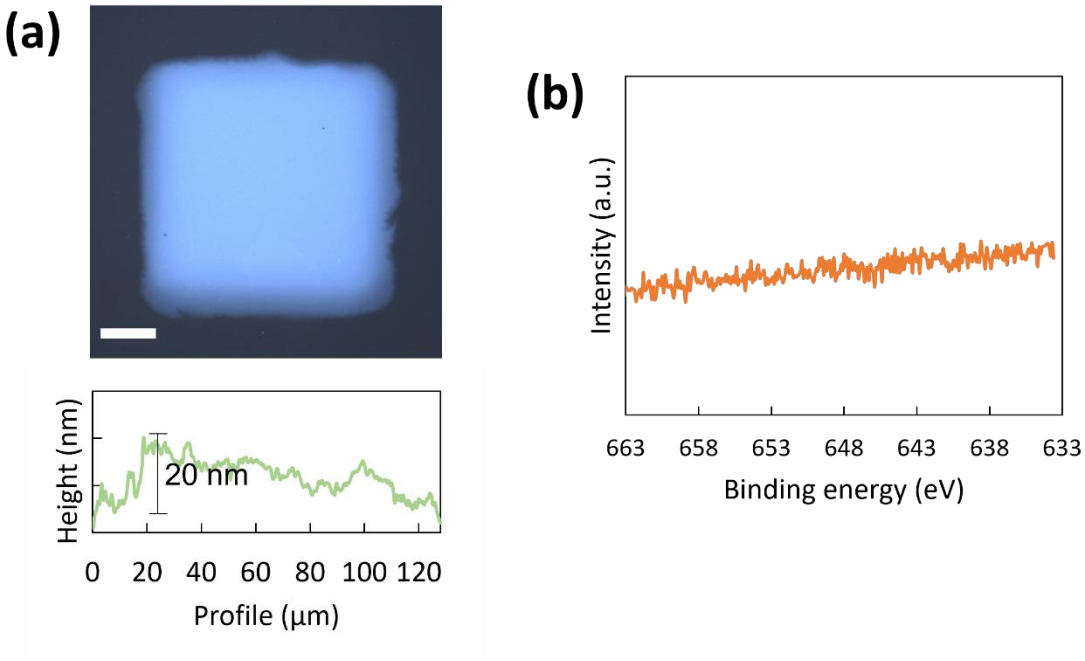

Figure S11. Photodeposition of MnO_x on Cr_2O_3/SiO_2. Laser microscope image (scale bar: 20 µm) at 100x magnification (a) and XPS spectrum of Mn 2p (b) after 20 hours photodeposition.

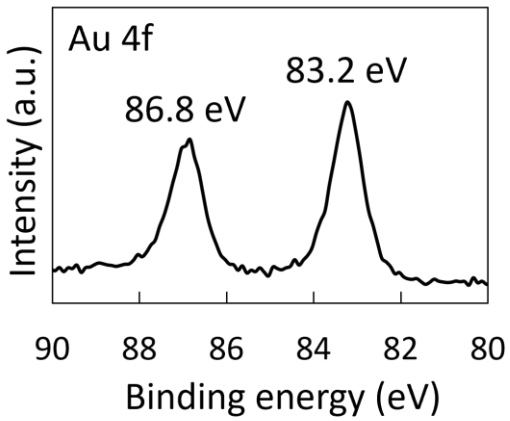

Figure S12. XPS spectrum of Au 4f from the photodeposited Au.

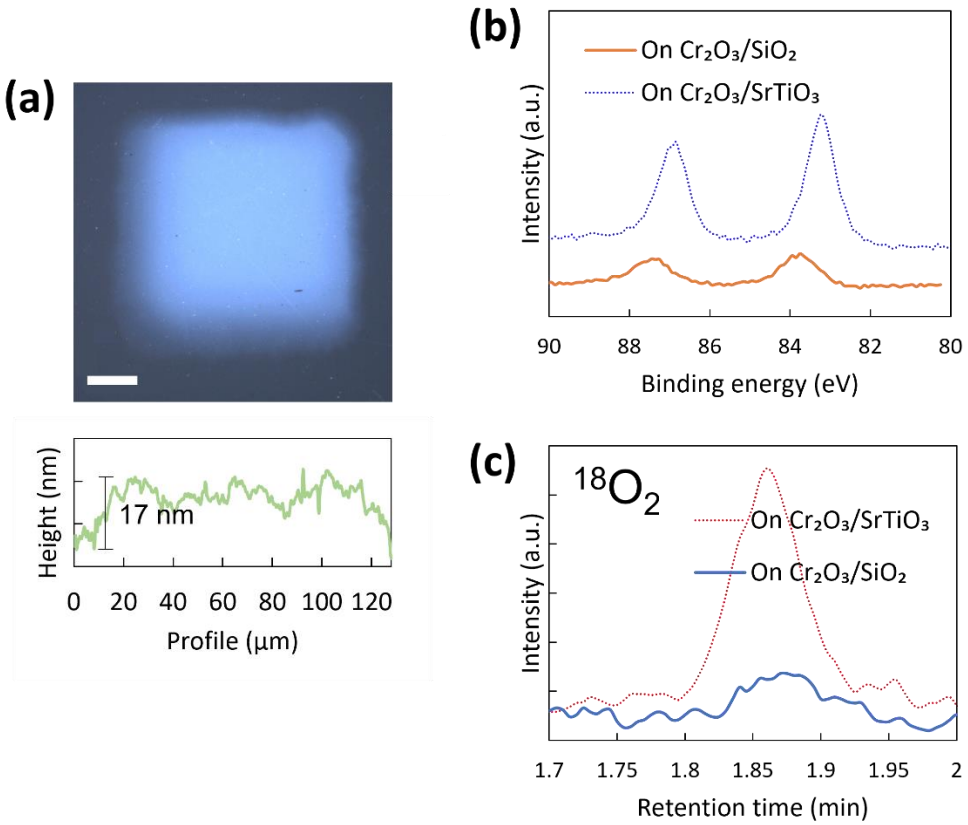

Figure S13. Photodeposition of Au on Cr_2O_3/SiO_2. Laser microscope image (scale bar: 20 µm) at 100 x magnification (a) after 20 hours photodeposition. Comparison of the Au 4f XPS spectrum (b) from the photodeposited Cr_2O_3/SiO_2 and $Cr_2O_3/SrTiO_3$. Photocatalytic oxygen evolution ($^{18}O_2$) during Au photodeposition (c) on Cr_2O_3/SiO_2 and $Cr_2O_3/SrTiO_3$. Water isotope ($H_2{}^{18}O$) was used for the analysis.

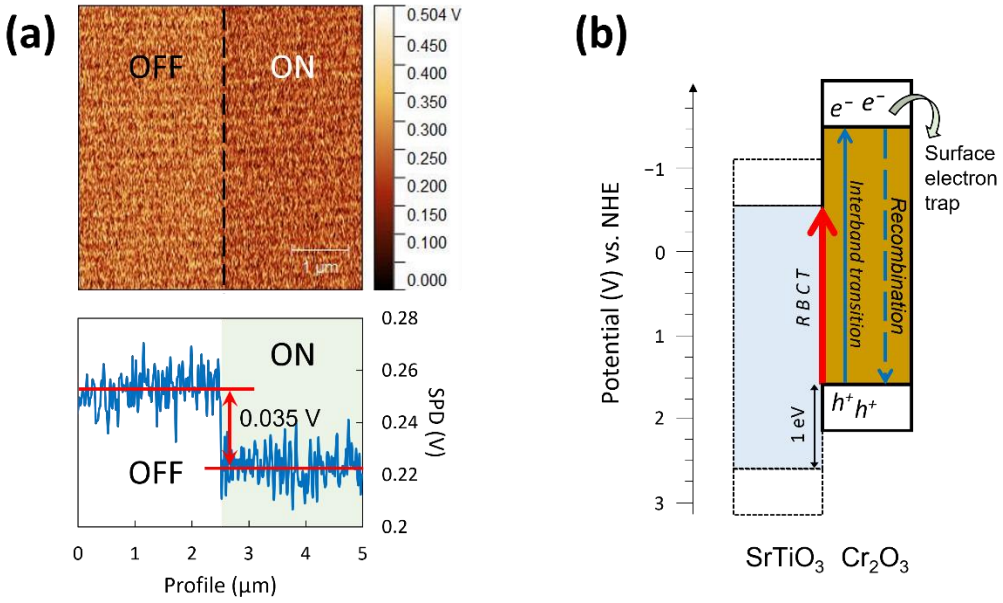

Figure S14. (a) Surface potential mapping on 3 nm Cr_2O_3/$SrTiO_3$ under light off and on with the absolute value of SPD_{on-off} of 0.035 V. The light source used in this case was a UV LED (365 nm). (b) Possible mechanism for the generation of the low SPD_{on-off} under the UV irradiation.

Figure S14a shows that the absolute value of SPD_{on-off} resulting from 365 nm (0.035 V) was lower than that of 405 nm and 470 nm irradiation (0.180 V and 0.078 V, respectively, as shown in Figure 3c, main manuscript), which indicated the suppression of holes generation on the surface of the Cr_2O_3 thin film. Under the UV irradiation, both $SrTiO_3$ and Cr_2O_3 were excited via inter-band transition in addition to the IFCT excitation. The inter-band transition of Cr_2O_3 causes electrons in the conduction band of Cr_2O_3, which would be recombined with holes in the valence band of Cr_2O_3 and/or trapped at surface sites of Cr_2O_3 (Figure S14b). Consequently, the generation of electrons in Cr_2O_3 under UV irradiation decreased the hole signal of the film. At present, the effect from the excited $SrTiO_3$ under UV irradiation is not clear, thus we only explained the sum of charge generation on the surface of the thin film.

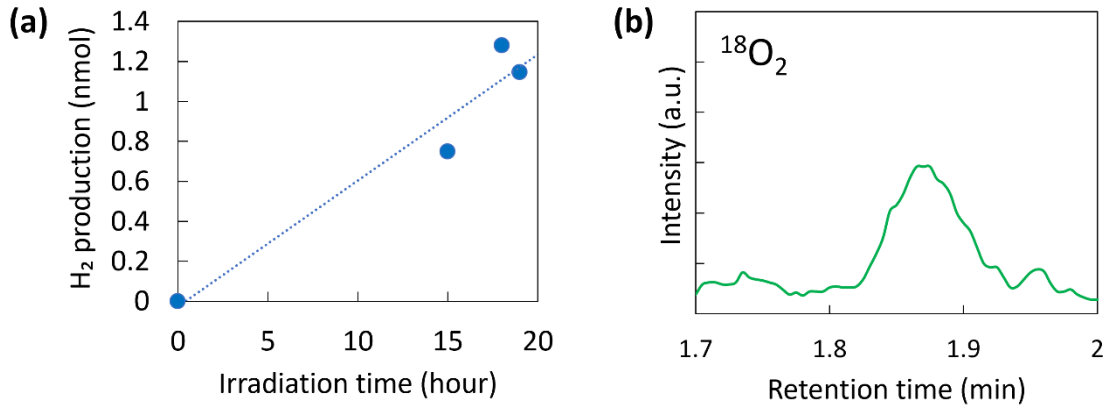

Figure S15. Photocatalytic water splitting activity on $Cr_2O_3/SrTiO_3$ after the photodeposition of Au and MnO_x. The produced hydrogen (a) was detected by GC-BID, while the evolved $^{18}O_2$ after 16 h (b) was monitored by GC-MS.

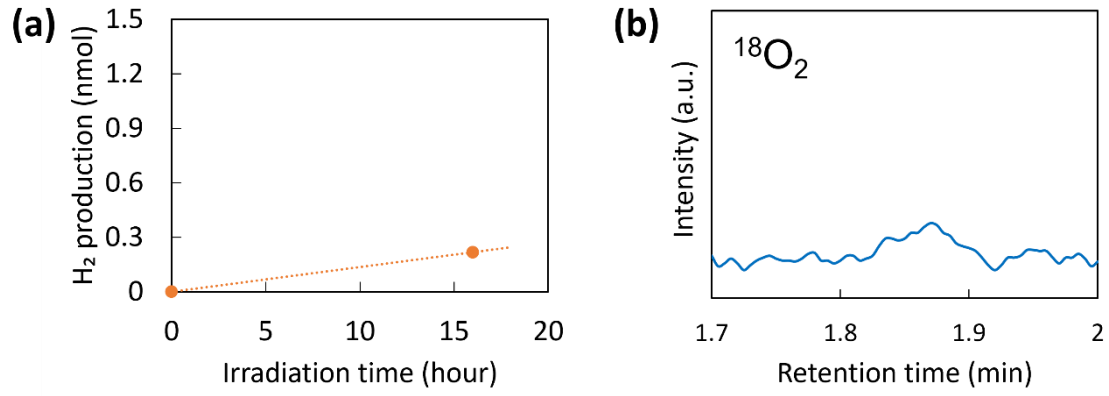

Figure S16. Photocatalytic water splitting activity on $Cr_2O_3/SrTiO_3$ after the photodeposition of Au. The evolved hydrogen (a) and oxygen-18 ($^{18}O_2$) (b) after 16h are presented.

Reference

1 M. Ebihara, T. Ikeda, S. Okunaka, H. Tokudome, K. Domen and K. Katayama, *Nat. Commun.*, 2021, **12**, 1–9.

2 H. Tan, Z. Zhao, W. Bin Zhu, E. N. Coker, B. Li, M. Zheng, W. Yu, H. Fan and Z. Sun, *ACS Appl. Mater. Interfaces*, 2014, **6**, 19184–19190.

3 V. E. Henrich, G. Dresselhaus and H. J. Zeiger, *Phys. Rev. B*, 1978, **17**, 4908–4921.

4 K. Osako, K. Matsuzaki, T. Susaki, S. Ueda, G. Yin, A. Yamaguchi, H. Hosono and M. Miyauchi, *ChemCatChem*, 2018, **10**, 3666–3670.

5 K. Osako, K. Matsuzaki, H. Hosono, G. Yin, D. Atarashi, E. Sakai, T. Susaki and M. Miyauchi, *APL Mater.*, 2015, **3**, 104409.